EAST EUROPEAN JOURNAL OF PHYSICS. **1.** 32-39 (2022)
DOI:10.26565/2312-4334-2022-1-05 ISSN 2312-4334

STUDY OF ELECTROSTATIC ION-CYCLOTRON WAVES IN MAGNETOSPHERE OF URANUS†

Rama S. Pandey[a], Mukesh Kumar[b,#]
[a]*Department of Applied Physics, Amity Institute of Applied Science, Amity University Noida UP India*
[b]*Department of Physics, Nalanda College Biharsharif Nalanda MU Bodh Gaya Bihar, India*
**Corresponding Author: rspandey@amity.edu*
[#]*E-mail: mukeshkumarpawapuri@gmail.com*
Received January 18, 2022; revised February 22, 2022; accepted March 1, 2022

In this manuscript, the method of characteristics particle trajectories details used and the dispersion relation for the ionosphere of Uranus were being used to investigate electrostatic ion-cyclotron waves with parallel flow velocity shear in the presence of perpendicular inhomogeneous DC electric field and density gradient. The growth rate has been calculated using the dispersion relation. Electric fields parallel to the magnetic field transmit energy, mass, and momentum in the auroral regions of the planetary magnetosphere by accelerating charged particles to extremely high energies. The rate of heating of plasma species along and perpendicular to the magnetic field is also said to be influenced by the occurrence of ion cyclotron waves and a parallel electric field in the acceleration area.
Keywords: Electrostatic Ion-cyclotron waves, Velocity shear, density gradient and Inhomogeneous Electric Field, Magnetosphere/Ionosphere of Uranus
PACS: 52.35Fp, 94.30Ch, 96.30Pj

The study of dynamics, which determines the release of free energy, has recently received a lot of attention. Its shear flow is determined by magneto hydrodynamics and plasma physics. The study of dynamics that govern the release of free energy associated with sheared flows has recently garnered a lot of attention in magnetohydrodynamics and plasma physics. In space plasma, sheared flows are ubiquitous, especially around the magnetopause, magnetospheric boundary layer, solar wind stream-stream interactions, comet tails, and the auroral ionosphere. Lemons et al. [1] used a kinetic technique to look at shearing velocity flow perpendicular to a uniform magnetic field for the electrostatic ion-cyclotron (EIC) instability. Simulations of ion-cyclotron waves in a magnetoplasma with transverse inhomogeneous electric field were employed in conjunction with Maxwellian plasma. Using Voyager 2's onboard plasma wave receiver, identical electrostatic ion-cyclotron waves were observed in Uranus' magnetosphere. A minor offset in the occurrence of electrostatic waves from the equator was predicted due to the substantial tilt of Uranian magnetic moment with respect to the planet's rotational axis. The most intense electrostatic waves were discovered around the magnetic equator, at a distance of roughly $11.5R_U$, according to reported measurements [2,3].

Because of the coupling of the zone of positive and negative energy of ion waves, Ganguli et al. [4,5] and Nishikawa et al. [6] argued that electrostatic waves with repetition of the request for ion-cyclotron frequencies can be unpredictable. Some researchers [7] have included the effect of parallel and perpendicular electric fields by modifying velocity terms appearing in the distribution function, actually results in an extension of earlier theory and obscuring the details of particle trajectories and with their effect. Others, using particle aspect investigation, have focused on the impact of an equal electric field on particle cyclotron instability for various distribution capacities. Others have used particle aspect analysis to investigate the effect of a parallel electric field on ion-cyclotron instability for various distribution functions [8,9]. Kandpal, et al.[10] investigated the Kelvin-Helmholtz instability in the magnetosphere of Saturn using an inhomogeneous DC electric field. With an inhomogeneous DC electric field, Kandpal and Pandey [11] explored higher harmonics electrostatic ion cyclotron parallel flow velocity shear instability in the magnetosphere of Saturn. The effect of different parameters on the growth rate of waves has been demonstrated using EIC instability and parallel velocity shear in the presence of an electric field perpendicular to the magnetic field [12].

The dielectric permittivity tensor of a magneto active current-driven plasma has been obtained by employing the kinetic theory based on the Vlasov equation and Lorentz transformation formulas with an emphasize on the q-nonextensive statistics for low frequency wave by Niknam [13]. Niyat et al [14] has solved dispersion relation for magnetized plasmas that has non-extensive electrons drifting with respect to stationary ions, and satisfies the other conditions for the excitation of electrostatic ion cyclotron waves using the standard linear Vlasov theory and q-distributions. The Electrostatic Ion Cyclotron (EIC) instability that includes the effect of wave-particle interaction has been studied owing to the free energy source through the flowing velocity of the inter-penetrating plasmas by Bashir et al [15]. The electrostatic waves in magnetized plasmas have been derived in the context of the nonextensive q-distribution of Tsallis statistics by Sharifi [16].

An ion beam propagating through collisional magnetized plasma containing electrons and two positive ion components has been discussed electrostatic ion cyclotron (EIC) instability via Cerenkov interaction [17]. Liu et al [18]

† ***Cite as***: R.S. Pandey, and M. Kumar, East. Eur. J. Phys. **1**, 32 (2022), https://doi.org/10.26565/2312-4334-2022-1-05

has explained the dispersive Alfvén wave in a low β plasma with anisotropic superthermal particles modeled by a bi-nonextensive distribution is derived from a kinetic theory. The effect of anisotropic temperature on inertial Alfvén wave is so small that it is negligible. The numerical results reveal that the presence of superthermal electrons in the small wavenumber limit will lead the damping rate of the kinetic Alfven wave (KAW) bigger than the one with Maxwellian distribution.

The experimental studies on electrostatic ion-cyclotron waves (EICWs) and their instability were often performed in a narrow plasma column in Q-machines, in which the wave was conventionally generated via the instability driven by an electron current parallel to a magnetic field. The propagation characteristics of wave patterns have seldom been studied, especially the different characteristics in pulse and continuous wave patterns [19]. Accumulation of carbon dioxide in the Earth's atmosphere leads to an increase in the greenhouse effect and, as a consequence, to significant climate change. Thus, the demand to develop effective technologies of carbon dioxide conversion grows year to year. Additional reason for research in this direction is the intention of Mars exploration, since 96% of the Martian atmosphere is just carbon dioxide, which can be a source of oxygen, rocket fuel, and raw materials for further chemical utilization. The enhancement of negative ion production in a volume Penning based source could be performed by the application of metal hydride cathode. Hydrogen isotopes are stored there in a chemically bound atomic state and desorbed from the metal hydride under the discharge current impact [20,21].

The dispersion equation has been derived on an approximation based for the current from the exact solutions of the characteristic cylindrical geometry form of the Vlasov plasma equation in a uniform magnetized plasma cylinder surrounded by a larger metal boundary outside a vacuum gap, which thus differs from that in unbounded plasmas by Kono et al [22].

Bashir et al [23] has studied the Bernstein mode instability driven by a perpendicular momentum ring distribution function is insensitive to the parallel distribution. However, in the relativistic treatment, owing to the inexorable coupling between the parallel and perpendicular momenta through the Lorentz factor, the parallel momentum distribution may affect the instability. Bashir and Vranjes [24] has studied the unstable kinetic drift wave in an electron-ion plasma can very effectively be suppressed by adding an extra flowing ion (or plasma) population. Theoretical study of the effects of positron density on the electrostatic ion cyclotron instability in an electron-positron-ion plasma using the kinetic theory approach by assuming that positrons and electrons can drift parallel to the magnetic field either in the same or the opposite directions has been studied by Khorashadizadeh et al [25].

The evolution of Fila mentation instability in a weakly ionized current-carrying plasma with nonextensive distribution has been studied in the diffusion frequency region, taking into account the effects of electron-neutral collisions Using the kinetic theory, Lorentz transformation formulas by Khorashadizadeh[26].The dispersion relation for parallel propagating waves in the ion-cyclotron branch has investigated numerically by considering that the velocity distribution of the ion population is a function of type product-bi-kappa. We investigate the effects of the non-thermal features and of the anisotropy associated with this type of distribution on the ion-cyclotron instability, as well as the influence of different forms of the electron distribution, by considering Maxwellian distributions, bi-kappa distributions, and product-bi-kappa distributions [27].

Incorporating the details of particle trajectories in the presence of non-uniform electric field and using them for bi-Maxwellian hot plasma to the magnetic field with velocity shear flow parallel to density gradient perpendicular to magnetic field, a conceptual study of ion-cyclotron instability has been performed for the magnetosphere of Uranus.

DISPERSION RELATION AND GROWTH RATE

Small perturbations in B_1, f_{s1} and E_1 linearize the Vlasov-Maxwell equations for homogeneous plasma, yielding the dispersion relation. The harmonic dependency of these perturbed quantities is assumed to be as. The following are the linearized first order Vlasov equations:

$$\frac{\partial f_{s1}}{\partial t} + \mathbf{V}.\frac{\partial f_{s1}}{\partial r} + \left(\frac{\mathbf{F}_s}{m_s}\right)\left(\frac{\partial f_{s1}}{\partial \mathbf{v}}\right) = S_s(r,v,t) \tag{1}$$

The term Force can be calculated as

$$\mathbf{F}_s = e_s\left[\mathbf{E}_o(x) + (\mathbf{v}\times\mathbf{B}_o)/c\right] \tag{2}$$

$$S_s(\mathbf{r},\mathbf{v},t) = \left(-\frac{e_s}{m_s}\right)\left[\mathbf{E}_1 + (\mathbf{v}\times\mathbf{B}_1)/c\right]\left(\frac{\partial f_{so}}{\partial \mathbf{v}}\right) \tag{3}$$

Where's' stands for species. The perturbed distribution function f_{s1}, which is derived from eq. (1), is calculated using the typical solutions approach.

$$f_{s1}(\mathbf{r},\mathbf{v},t) = \int_{-\infty}^{0} S_s\left[\mathbf{r}_0(\mathbf{r},\mathbf{v},t),\mathbf{v}_0(\mathbf{r},\mathbf{v},t),t-t'\right]dt$$

The phase space coordinate system has undergone a transformation. From $(\mathbf{r},\mathbf{v},t)$ to $(\mathbf{r}_0,\mathbf{v}_0,t-t')$ where $t-t'=\tau$ The particle trajectories for the inhomogeneous external DC electric field and the homogeneous magnetic field, as specified by [28], are as follows:

$$\mathbf{x}(\tau) = x_0 + \frac{\mathbf{v}_\perp}{\Omega_s}\left(1+\frac{\bar{\mathbf{E}}'(x)}{4\Omega_s^2}\right)\left[\sin(\theta-\Omega_s\tau)-\sin\theta\right]$$

$$\mathbf{y}(\tau) = y_0 + \Delta' + \frac{\mathbf{v}_\perp}{\Omega_s}\left(1+\frac{3}{4}\frac{\bar{\mathbf{E}}'(x)}{4\Omega_s^2}\right)\left[\cos(\theta-\Omega_s\tau)-\cos\theta\right]$$

$$\mathbf{z}(\tau) = \mathbf{z}_0 + \mathbf{v}_\parallel\tau \tag{5}$$

Where

$$\Delta = \frac{\bar{\mathbf{E}}'(x)\tau}{\Omega_s}\left[1+\frac{\mathbf{E}''(x)}{\mathbf{E}(x)}.\frac{1}{4}\left(\frac{\mathbf{v}_\perp}{\Omega_s}\right)^2+....\right]$$

$$\bar{\mathbf{E}}(x) = \frac{e_s\mathbf{E}(x)}{m_s} \text{ and } \mathbf{E}(x) = \mathbf{E}_{0x}\left(1-\frac{x^2}{a^2}\right)$$

So, $\bar{\mathbf{E}}'(x) = \dfrac{e_s\mathbf{E}_{ox}(1-\rho)}{m_s}$

where $\rho = \dfrac{2x}{a^2}$ and $\Omega_s = \dfrac{e_s\mathbf{B}_o}{m_s}$

After replacing the unperturbed trajectories in equation (4) and followed by simplified algebraic calculations following technique out lined in [11] the perturbed distribution function based on time integration is given as:

$$f_{s1}(\mathbf{r},\mathbf{v},t) = \sum_s^{e,i}\frac{ie_s}{m_s\omega}\sum_{m,n,p,g}J_n(\lambda_1)J_m(\lambda_1)J_p(\lambda_2)J_g(\lambda_2)e^{i(m-n)(\pi/2+\theta)}.e^{i(g-p)(\pi/2+\theta)}\frac{\left[\mathbf{E}_{1x}U^*+\mathbf{E}_{1y}V^*+\mathbf{E}_{1z}W^*\right]}{k_\parallel\mathbf{v}_\parallel+n\Omega_s+p\Omega_s+k_\perp\Delta'-\omega} \tag{6}$$

where

$$U^* = C\mathbf{v}_\perp\frac{n}{\lambda_1}\left(1-\frac{\bar{\mathbf{E}}'(x)}{4\Omega_s^{\,2}}\right)+k_\perp\mathbf{v}_\perp\zeta''\frac{n}{\lambda_1}\left(1+\frac{\bar{\mathbf{E}}'(x)}{4\Omega_s^{\,2}}\right)$$

$$V^* = iC\mathbf{v}_\perp\frac{J_n'}{J_n}+\frac{3}{4}C\mathbf{v}_\perp\frac{n}{\lambda_1}\frac{\bar{\mathbf{E}}'(x)}{4\Omega_s^{\,2}}-C\Delta'$$

$$W^* = \omega\frac{\delta f_{so}}{\delta v_\parallel}+Dk_\perp\mathbf{v}_\perp\frac{n}{\lambda_1}+\frac{3}{4}Dk_\perp\mathbf{v}_\perp\frac{n}{\lambda_1}\frac{\bar{\mathbf{E}}'(x)}{\Omega_s^{\,2}}+k_\perp\mathbf{v}_\parallel\Delta'+k_\perp\mathbf{v}_\parallel\zeta''$$

$$C = \left(\omega-k_\parallel\mathbf{v}_\parallel\right)\left(\frac{-2f_{so}}{\alpha_{\perp s}^2}\right)+k_\parallel\frac{\delta f_{so}}{\delta\mathbf{v}_\parallel}$$

$$D = \mathbf{v}_\parallel\left(\frac{-2f_{so}}{\alpha_{\perp s}^2}\right)-\frac{\delta f_{so}}{\delta\mathbf{v}_\parallel} \tag{7}$$

$$\lambda_1 = \frac{k_\perp\mathbf{v}_\perp}{\omega_{cs}}, \qquad \lambda_2 = \frac{3}{4}\frac{k_\perp\mathbf{v}_\perp\bar{\mathbf{E}}'(x)}{\Omega_s^3}, \qquad \Delta' = \frac{\delta\Delta}{\delta t}$$

Δ is the series variation of inhomogeneous electric field and Δ' is the time derivative of Δ The unperturbed bi-Maxwellian distribution function can be written by Huba (29):

$$f_{so} = f_{mo} + v_y\zeta''$$

$$\zeta'' = \frac{1}{\Omega_s}\left[\varepsilon_n+\frac{2\left(\mathbf{v}_\parallel-\mathbf{v}_{oz}(x)\right)}{\alpha_{\parallel s}^2}\frac{\delta v_{oz}(x)}{\delta x}\right]f_{mo}$$

$$f_{mo} = \frac{n_o(x)}{\pi^{3/2}\alpha_{\perp s}^2\alpha_{\parallel s}}\exp\left[-\frac{\left(\mathbf{v}_{ox}^2+\mathbf{v}_{oy}^2\right)}{\alpha_{\perp s}^2}-\frac{\left(\mathbf{v}_\parallel-v_{oz}(x)\right)^2}{\alpha_{\parallel s}^2}\right]$$

Where ζ'' is being constant of motion:

$$\alpha_{\perp,\|s} = \sqrt{\frac{2K_b T_{\perp,\|s}}{m_s}} \tag{8}$$

Where ζ'' is being constant of motion and K_b is the Maxwell Boltzmann constant

Now making it easy by replacing m=n, g=p and applying the standard definition of conductivity and current density, the dielectric tensor can be calculated as:

$$\left\|\varepsilon(k,\omega)\right\| = 1 - \sum_{s}^{e,i} \frac{4e_s^2\pi}{m_s\omega^2} \int \sum_{n,p} J_p^2(\lambda_2) \frac{d^3\mathbf{v} \sum_{i,j}^{x,y,z} \|S_{ij}\|}{k_\| \mathbf{v}_\| + n\Omega_s + p\Omega_s + k_\perp \Delta' - \omega} \tag{9}$$

$$\text{Where, } \|S_{ij}\| = \begin{vmatrix} \mathbf{v}_\perp J_n^2 \frac{n}{\lambda_1} U^* & J_n^2 \mathbf{v}_\perp \frac{n}{\lambda_1} V^* & \mathbf{v}_\perp J_n^2 \frac{n}{\lambda_1} W^* \\ -i\mathbf{v}_\perp J_n' J_n U^* & -i\mathbf{v}_\perp J_n^2 V^* & i\mathbf{v}_\perp J_n^2 W^* \\ \mathbf{v}_\| J_n^2 U^* & \mathbf{v}_\| J_n^2 V^* & \mathbf{v}_\| J_n^2 W^* \end{vmatrix} \tag{10}$$

Now we consider electrostatic ion-cyclotron instability

$$\|\varepsilon_{xx}\| = N^2 \tag{11}$$

Here N represents the index of refraction.

The estimating method can be used to obtain the final electrostatic dispersion relation of Huba [29] and combining equation (8), (9), (10) and (11)

$$D(k,\omega) = 1 + \sum_{s}^{e,i} \frac{2\omega_{ps}^2}{k_\perp^2 \alpha_{\perp s}^2} \sum_{n,p} \Gamma_n(\mu_s) \sum J_p^2(\lambda_2) \left(1 - \frac{\bar{\mathbf{E}}'(x)}{4\Omega_s^2}\right) \cdot \frac{k_\perp}{k_\|} \left[\left(\frac{\bar{\omega}}{k_\| \alpha_{\|s}} - \frac{1}{2}\varepsilon_n \rho_s \frac{\alpha_{\perp s}}{\alpha_{\|s}} \right) Z(\zeta) + \right.$$
$$\left. + A_T \frac{k_\|}{k_\perp} \left(1 + \zeta Z(\zeta)\right) - A_s \left(\frac{\alpha_{\perp s}}{\alpha_{\|s}} \right)^2 \left(1 + \zeta Z(\zeta)\right) \right] \tag{12}$$

$Z(\zeta) = (\pi)^{-\frac{1}{2}} \int_{-\infty}^{\infty} \frac{e^{-t^2}}{t - \zeta}\, dt$ is plasma dispersion function with ζ given as:

$$\zeta = \frac{\bar{\omega} - (n+p)\Omega_s - k_\perp \Delta'}{k_\| \alpha_{\|s}}$$

$$A_s = \frac{1}{\Omega_s} \frac{\delta \mathbf{v}_{oz}(x)}{\delta x}$$

$$A_T = \frac{\alpha_{\perp s}^2}{\alpha_{\|s}^2} - 1$$

$$\varepsilon_n = \frac{\delta \ln n(x)}{\delta x}, \qquad \bar{\omega} = \omega - k_\| \mathbf{v}_{oz}(x) \tag{13}$$

$$\mu_s = \frac{k_\perp^2 \rho_i^2}{2}, \qquad \lambda_{DS}^2 = \frac{\alpha_{\perp s}^2}{2\omega_{ps}^2}$$

ω_{ps}^2 = Squared of plasma frequency

Where $Z(\zeta)$ represents plasma dispersion function

Now the above-mentioned dispersion relation comes to a final form to that of Huba [29] by the removal of inhomogeneous DC electric field is removed from the equation, and $\alpha_{\perp s} = \alpha_{\|s}$, and based on [29] assumptions for p = 0 and s = i, e. The assumption is used to estimate the dispersion relation for electrons and ion approximations. $k_\perp \rho_e << 1$ and there is no such approximation for ions. Thus equation (12) is simplified as:

$$D(k,\omega) = 1 + \frac{1}{k_\perp^2 \lambda_{De}^2} \eta_e \frac{T_{\perp e}}{T_{\|e}} + \frac{1}{k_\perp^2 \lambda_{Di}^2} \eta_i \left[\frac{T_{\perp i}}{T_{\|i}} \Gamma_n(\mu_i) \frac{k_\perp}{k_\|} \left[\left(\frac{\bar{\omega}}{k\alpha_\|} \frac{T_{\perp i}}{T_{\|i}} - \frac{1}{2}\varepsilon_n \rho_i \frac{\alpha_{\perp i}}{\alpha_{\|i}} + \frac{\left(n\Omega_i + k_\perp \Delta'\right)}{k_\| \alpha_{\|i}} \right.\right.\right.$$
$$\left.\left.\left. \times \left(1 - \frac{T_{\perp i}}{T_{\|i}}\right)\right) Z(_i) - A_i \frac{T_{\perp i}}{T_{\|i}} \left(1 + \zeta Z(\zeta_i)\right) \right] \right] \tag{14}$$

After substituting $Z(\zeta_i) = -\frac{1}{\zeta_i} - \frac{1}{2\zeta_i^3}$, $n_{oi} = n_{oe}$ and multiplying throughout with $\frac{k_\perp^2 \lambda_{Di}^2}{\eta_i}$

$$0 = \frac{\lambda_{Di}^2}{\lambda_{De}^2}\frac{\eta_e}{\eta_i}\frac{T_{\perp e}}{T_{\| e}} + \left[\frac{T_{\perp i}}{T_{\| i}} - \Gamma_n(\mu_i)\frac{T_{\perp i}}{T_{\| i}} + \frac{\Gamma_n(\mu_i)k_\perp}{2k_\|}\varepsilon_n\rho_i\frac{\alpha_{\perp i}}{\alpha_{\| i}}\cdot\frac{k_\|\alpha_{\| i}}{\bar{\omega} - n\Omega_i + k_\perp\Delta'} - \frac{\Gamma_n(\mu_i)k_\perp}{k_\|}\times\right.$$
$$\left.\times\frac{n\Omega_i + k_\|\alpha_{\| i}}{\bar{\omega} - n\Omega_i + k_\perp\Delta'} - \frac{\Gamma_n(\mu_i)}{2(\bar{\omega} - n\Omega_i + k_\perp\Delta')^2}\cdot\frac{T_{\perp i}}{T_{\| i}}(k_\|\alpha_{\| i})^2\left(1 - \frac{k_\perp}{k_\|}A_i\right)\right] \quad (15)$$

$$\eta_e = 1 - \frac{\bar{E}_e'(x)}{4\Omega_e^2}$$

$$\eta_i = 1 - \frac{\bar{E}_i'(x)}{4\Omega_i^2}$$

Multiplying equation (15) throughout by $\left(\frac{\bar{\omega} - n\Omega_i + k_\perp\Delta'}{k_\|\alpha_{\| i}}\right)^2$ we obtain a quadratic dispersion equation as:

$$a_1\left(\frac{\bar{\omega}'}{\Omega_i}\right)^2 + b_1\left(\frac{\bar{\omega}'}{\Omega_i}\right) + c_1 = 0 \quad (16)$$

where

$$a_1 = a_2\left(\frac{\Omega_i}{\alpha_{\| i}k_\|}\right)^2$$

$$a_2 = \frac{T_{\perp i}}{T_{\| e}}\frac{\eta_e}{\eta_i} + \frac{T_{\perp i}}{T_{\| i}} - \Gamma_n(\mu_i)\frac{T_{\perp i}}{T_{\| i}}$$

$$b_1 = b_2\left(\frac{\Omega_i}{\alpha_{\| i}k_\|}\right) - \frac{2k_\perp\Delta' a_2\Omega_i}{\alpha_{\| i}^2 k_\|^2}$$

$$b_2 = \frac{k_\perp}{2k_\|}\frac{\Gamma_n(\mu_i)\varepsilon_n\rho_i\alpha_{\perp i}}{\alpha_{\| i}} - \Gamma_n(\mu_i)\frac{k_\perp}{k_\|} - \Gamma_n(\mu_i)\frac{k_\perp n\Omega_i}{\alpha_{\| i}k_\|^2}$$

$$c_1 = \frac{\Gamma_n(\mu_i)T_{\perp i}}{2T_{\| i}}\left(1 - \frac{k_\perp}{k_\|}A_i\right) - \frac{b_2k_\perp\Delta'}{\alpha_{\| i}k_\|} + \frac{a_2k_\perp^2(\Delta')^2}{\alpha_{\| i}^2k_\|^2} \quad (17)$$

$\bar{\omega}' = \bar{\omega} - n\Omega_i$

The solution of equation (16) is

$$\bar{\omega}' = -\frac{b_1}{2a_1}\left[1 \mp \left(1 - \frac{4a_1c_1}{b_1^2}\right)^{1/2}\right] \quad (18)$$

From this expression growth rate has been calculated by computer analysis when $b_1^2 << 4a_1c_1$. This criteria gives a condition for the growth of wave when

$$A_i > \frac{k_\|}{k_\perp}\left[1 - \frac{2T_{\| i}}{\Gamma_n(\mu_i)T_{\perp i}}\left(\frac{\left(\frac{b_2\Omega_i}{\alpha_{\| i}k_\|} - \frac{2a_2k_\perp\Omega_i\Delta'}{\alpha_{\| i}^2k_\|^2}\right)^2}{4a_2\left(\frac{\Omega_i}{\alpha_{\| i}k_\|}\right)^2} + \frac{b_2k_\perp\Delta'}{\alpha_{\| i}k_\|} - \frac{a_2k_\perp^2(\Delta')^2}{\alpha_{\| i}^2k_\|^2}\right)\right]$$

In long wavelength limit when $k_\perp^2\rho_i^2 << 1$ and removal of non-uniform DC electric field for Maxwellian plasma $\alpha_{\perp i} = \alpha_{\| i}$

$$A_i > \frac{k_\|}{k_\perp}\left[1 + \frac{T_e}{T_i}\frac{k_\perp^2}{k_\|^2}(\varepsilon_n\rho_i)^2\right]$$

An expression close to that of Huba [29] is obtained.

PLASMA PARAMETERS

From Kurth etal [2] and Pandey [30] the following values of plasma properties for Uranus' magnetosphere, Growth rate (γ/ω_c) variations with $k_\perp\rho_i$were determined using equation (18):E_o= 1mV/m, B_o=11nT A_i = 0.05, $T_\perp/T_{||}$=1.25, ρ =0.5, T_e/T_i=4, $\varepsilon_n\rho_i$= 0.02 and θ = 89° at 11 R_U.

RESULTS AND DISCUSSION

Figure 1 shows the variation in growth rates in respect to $k_\perp\rho_i$ for assumed values of shear scale length (A_i) have been shown.

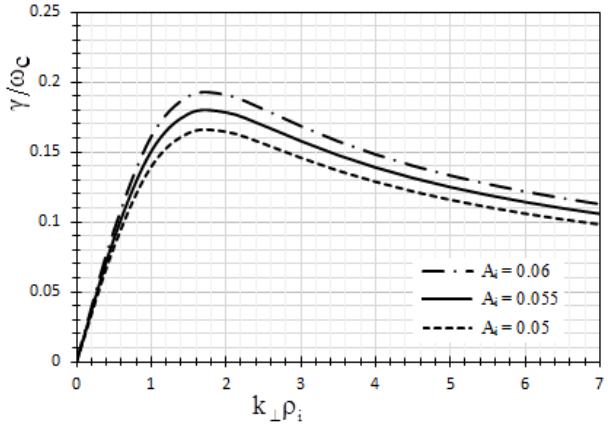

Figure 1. Differences in the rates of growth in relation to $k_\perp\rho_i$ for differing values of A_i at $T_\perp/T_{||}$=1.25, T_e/T_i=4, ρ =0.5, $\varepsilon_n\rho_i$=0.02, θ =89° and additional fixed plasma characteristics.

At harmonics n = 1 and A_i = 0.05, growth rate is 0.1645. Growth rate increases from 0.1783 to 0.1912 for A_i = 0.055 and 0.06 respectively. The maxima of growth rate occurs at $k_\perp\rho_i$= 1.8 in every case. The velocity shear ion-cyclotron like waves are excited for $k_\perp\rho_i$> 1 at shorter wavelength regions [5, 31], as shown in this chapter. Our results are similar to numerical simulation using M.H.D. equation valid at large ion larmor radius [32]. When the gyro radius is similar to the velocity shear scale length, the instability appears to have stabilized. Figure 2 represents the growth rate variation with respect to $k_\perp\rho_i$for diverse values of density scale length ($\varepsilon_n\rho_i$). The increases in growth rate with increasing value of density scale length, as for $\varepsilon_n\rho_i$= 0.02 and 0.08, growth rate increases from 0.1645 to 0.1758 with no change in $k_\perp\rho_i$= 1.8. Fujimoto and Terasawa [33] According to simulation data, the mixing efficiency of non-uniform background plasma is a function of density ratio, plasma, shear layer width, and growth mode wavelength. Their conclusion is supported by our findings. Figure 3 indicates the change in growth rate for the ion-cyclotron instability in Uranus' magnetosphere with harmonic n=1.

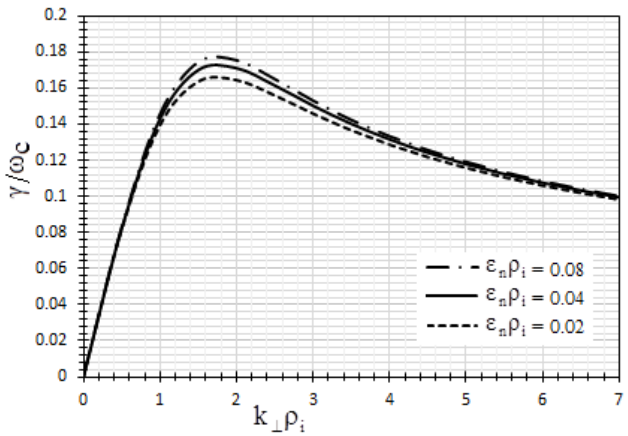

Figure 2. Differences in the rates of growth in relation to $k_\perp\rho_i$ for varying values of $\varepsilon_n\rho_i$ at $T_\perp/T_{||}$=1.25, T_e/T_i=4, ρ =0.5, A_i =0.05, θ =89° and additional fixed plasma characteristics.

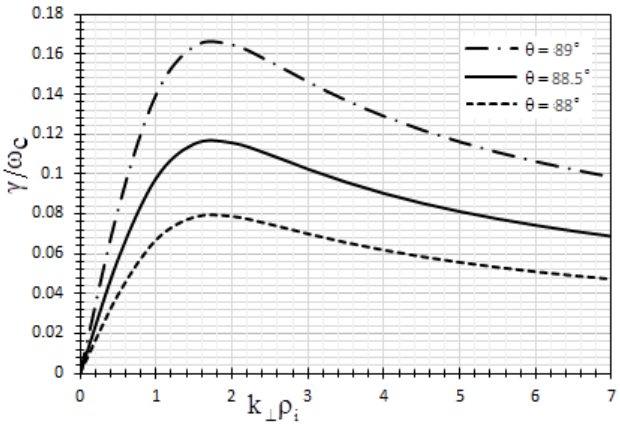

Figure 3. Differences in the rates of growth in relation to $k_\perp\rho_i$ for varying values of θ at $T_\perp/T_{||}$=1.25, T_e/T_i=4, ρ =0.5, A_i =0.05, $\varepsilon_n\rho_i$= 0.02 and additional fixed plasma characteristics.

For various values of propagation angle, the growth rate is confirmed with reference to the magnetic field angle (θ). The magnetic dipole axis, which is tilted at sixty degrees like Uranus' spin axis, condenses, resulting in a more bending magnetic field and magnetic field intersection [34,35]. In the graph, for θ =88°, γ/ω_c=0.0787, for

θ =88.5°, γ/ω_c=0.1156 and for θ =89°, γ/ω_c=0.1645. Therefore, it is concluded that even the slight lowering in angle of propagation decreases the growth rate significantly for Uranian magnetosphere. In Figure 4 variation of growth rate with $k_\perp\rho_i$for various values of electric field have been showed. For E_o= 1mV/m, maximum growth rate, γ/ω_c=0.1645 appears at $k_\perp\rho_i$=1.8 and for E_o = 0.1mV/m, maximum growth rate, γ/ω_c=0.1753 appears again at $k_\perp\rho_i$=1.8. At n=1 harmonic of ion cyclotron gyro frequency, growth rate reduces with higher value of electric field. This shows that increasing electric field magnitude has a stabilizing effect on electrostatic ion-cyclotron waves. The behavior is in accordance with Misra and Tiwari [8] this illustrates that the parallel electric field has the effect of stabilizing wave expansion and increasing ion transverse acceleration. Figure 5 shows the effect of varying T_e/T_ion growth rate of ion-cyclotron waves for 11 R_U, other fixed parameters as mentioned in figure caption.

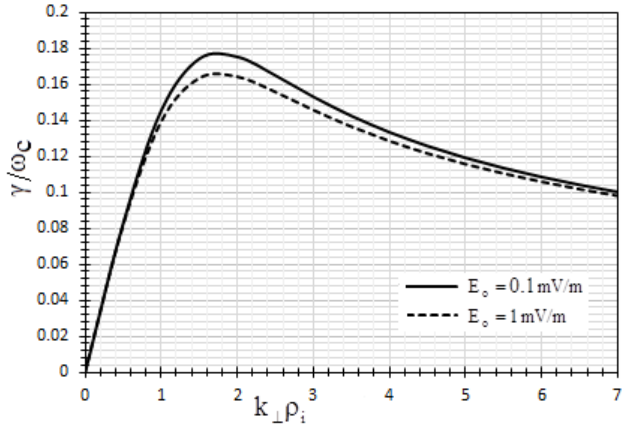

Figure 4. Differences in the rates of growth in relation to $k_\perp\rho_i$ for varying values of E_o at $T_\perp/T_{||}$=1.25, T_e/T_i=4, ρ =0.5, A_i =0.05, θ =89°, $\varepsilon_n\rho_i$= 0.02 and additional fixed plasma characteristics.

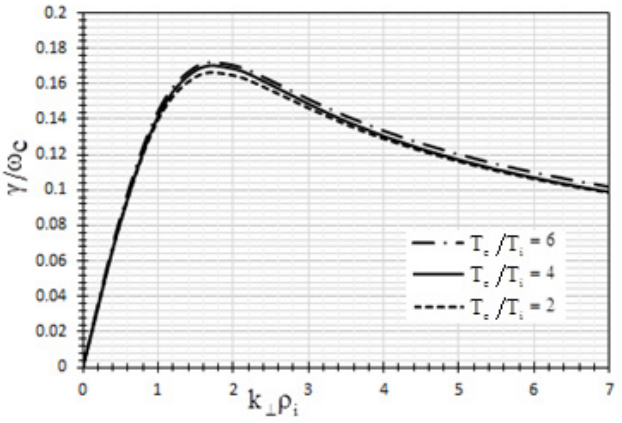

Figure 5. Differences in the rates of growth in relation to $k_\perp\rho_i$ for varying values of η_e/η_i at $T_\perp/T_{||}$=1.25, $\varepsilon_n\rho_i$= 0.02, ρ =0.5, A_i =0.05, θ =89° and additional fixed plasma characteristics.

With T_e/T_i= 2, 4 and 6, γ/ω_c= 0.1496, 0.1645 and 0.1705 respectively. It is seen that with increasing the value ofT_e/T_i, growth rate also increases. Figure 6 has been made to depict the diversity in growth rates with respect to $k_\perp\rho_i$for differing value of $\rho$and other parameters fixed. The effects of inhomogeneity non the electric field with a constant DC field magnitude are depicted in this diagram. The maximum growth rate increases from 0.1645 to 0.1722 as the value of increases from 0.5 to 0.9. Velocity shear ion-cyclotron like waves are excited in the regions where E x B drift is localized. The effect of non-uniform electric field in the perpendicular direction makes it to be a function of position as shown in the expression and thus cyclotron frequency is renormalized. In Figure 7 the variation of growth rate with relation to $k_\perp\rho_i$for varying values of ratio of perpendicular to parallel temperature ($T_\perp/T_{||}$) are shown. Since $T_\perp/T_{||}$-1 = A_T, the graph actually shows growth rate for different anisotropies (A_T). For $T_\perp/T_{||}$= 1.25, γ/ω_c= 0.1645, for $T_\perp/T_{||}$= 1.5, γ/ω_c= 0.1685 and for $T_\perp/T_{||}$=1.75, γ/ω_c= 0.1708. Thus, temperature anisotropy becomes an additional source along with velocity shear, density scale length and angle of propagation, for exciting shorter wavelengths. The results can be compared to Misra and Tiwari [8] for terrestrial magnetosphere.

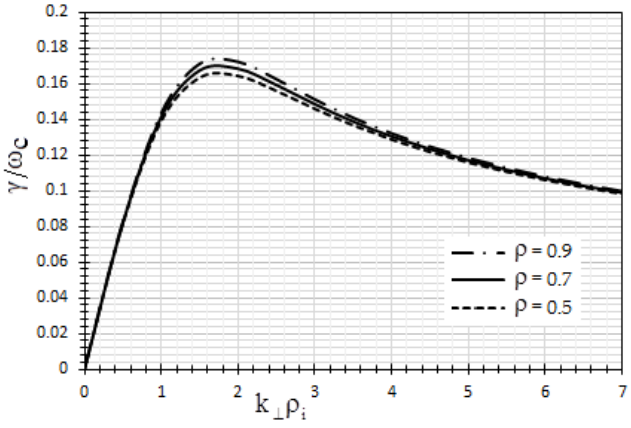

Figure 6. Differences in the rates of growth in relation to $k_\perp\rho_i$ for various values of ρ at $T_\perp/T_{||}$=1.25, T_e/T_i=4, $\varepsilon_n\rho_i$= 0.02, A_i =0.05, θ =89°and additional fixed plasma characteristics.

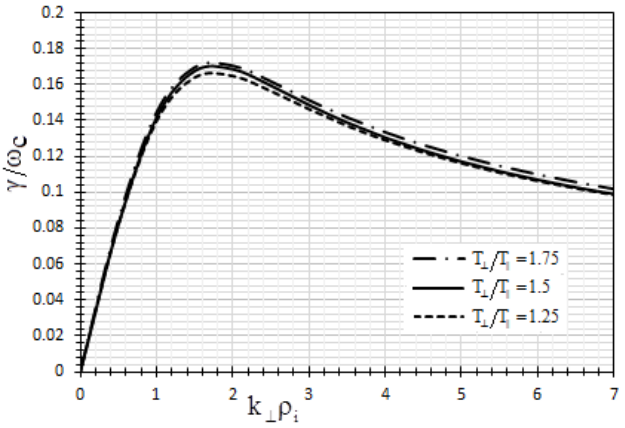

Figure 7. Differences in the rates of growth in relation to $k_\perp\rho_i$ for varying values of $T_\perp/T_{||}$ at $\varepsilon_n\rho_i$= 0.05, T_e/T_i=4, ρ =0.5, A_i =0.05, θ =89° and additional fixed plasma characteristics.

CONCLUSION

In the presence of a parallel DC field, this study shows the stimulation of electrostatic ion-cyclotron waves in Uranus' magnetosphere. The inclusion of temperature anisotropy and inhomogeneous electric field through kinetic approach leads to conclusion that in addition to driving sources of instability, such as temperature anisotropy and velocity shear, angle of propagation. In the case of the Uranian magnetosphere, it also has a significant impact on the rate of expansion of ion-cyclotron waves. The increase in electric field magnitude plays stabilizing effect on electrostatic ion-cyclotron instability, thus decreasing the growth rate of the waves as well as enhances transverse acceleration of ions.

ORCID IDs

Rama S. Pandey, https://orcid.org/0000-0003-4907-1080; **Mukesh Kumar,** https://orcid.org/0000-0001-6106-4794

REFERENCES

[1] D.S. Lemons D. Winske, and S.P. Gary, J. Geophys. Res. **97**, 19381 (1992). https://doi.org/10.1029/92JA01735
[2] W.S. Kurth, D.D. Barbosa, D.A. Gurnett, and F.L. Scarf, J. Geophys. Res. **92**(A13), 15225 (1987). https://doi.org/10.1029/ja092ia13p15225
[3] P. Zarka, Advances in Sp. Res. **33**, 2045 (2004). https://doi.org/10.1016/j.asr.2003.07.05
[4] G. Ganguli, and Y.C. Lee, Phys. Fluids, **28**, 761 (1985). https://doi.org/10.1063/1.865096
[5] G. Ganguli, Y.C. Lee, and P.J. Palmadesso, Phys. Fluids, **31**, 823 (1988). https://doi.org/10.1063/1.866818
[6] K.I. Nishikawa, G. Ganguli, Y.C. Lee, and P.J. Palmadesso, Phys. Fluids, **31**, 1568 (1988). https://doi.org/10.1063/1.866696
[7] G. Ganguli , Bakshi P. and Palmadesso P., J. Geophys. Res. **89**, 945 (1984). https://doi.org/10.1029/JA089iA02p00945
[8] R Misra. and Tiwari M.S., Planetary and Space Sci. **54** (2), 188 (2006). https://doi.org/10.1016/j.pss.2005.11.003
[9] G. Ahirwar, P. Varma and M.S.Tiwari, Annales Geophysicae, **24**(7), 1919 (2006). https://doi.org/10.5194/angeo-24-1919-2006
[10] P. Kandpal, R. Kaur, and R.S. Pandey, Advances in Space research, **61**, 581 (2018). https://doi.org/10.1016/j.asr.2017.09.033
[11] P. Kandpal, and R.S. Pandey, Astrophysics and Space Sciences, **363**, 227 (2018). https://doi.org/10.1007/s10509-018-3442-7
[12] R.K. Tyagi, K.K. Srivastava, and R.S. Pandey, Surface Engineering and Applied Electrochemistry, **47**(4), 370 (2011). https://doi.org/10.3103/S1068375511040144
[13] A.R. Niknam, E. Rastbood, and S.M. Khorashadizadeh, Phys. Plasmas, **22**, 122102 (2015). https://doi.org/10.1063/1.4936825
[14] M. Barati Moqadam Niyat, S.M.Khorashadizadeh and A.R. Niknam, Physics of Plasmas, **23**, 122110 (2016). https://doi.org/10.1063/1.4971810
[15] M.F. Bashir, R. Ilie, and G.Murtaza, Physics of Plasmas, **25**, 052114 (2018). https://doi.org/10.1063/1.5025843
[16] M. Sharifi, and A. Parvazian, Physica A, **393**, 489 (2014). https://doi.org/10.1016/j.physa.2013.09.024
[17] J. Sharma, S.C. Sharma, and D. Kaur Progress In Electromagnetics Research Letters, **54**, 123 (2015). https://doi.org/10.2528/PIERL15042703
[18] Y. Liu, Y.F. Wang, and T.P. Hu, Phys. Plasmas, **23**, 042103 (2016). https://doi.org/10.1063/1.4945635
[19] K.-Y. Yi, Z.A. Wei, J.X. Ma, Q. Liu, and Z.Y. Li, Physics of Plasmas, **27**, 082103 (2020). https://doi.org/10.1063/1.5144453
[20] I. Sereda, Ya. Hrechko, Ie. Babenko, East Eur. J. Phys. **3**, 81 (2021). https://doi.org/10.26565/2312-4334-2021-3-12
[21] V.A. Lisovskiy, S.V. Dudin, P.P. Platonov, and V.D. Yegorenkov, East Eur. J. Phys. **4**, 152 (2021). https://doi.org/10.26565/2312-4334-2021-4-20
[22] M. Kono, J. Vranjes, and N. Batool, Phys. Rev. Lett. **112**, 105001 (2014). https://doi.org/10.1103/PhysRevLett.112.105001
[23] M.F. Bashir, N. Noreen, G. Murtaza, and P.H. Yoon, Plasma Phys. Controlled Fusion, **56**, 055009 (2014). https://doi.org/10.1088/0741-3335/56/5/055009
[24] M.F. Bashir, and J. Vranjes, Phys. Rev. E, **91**, 033113 (2015). https://doi.org/10.1103/PhysRevE.91.033113
[25] S.M. Khorashadizadeh, M. Barati M. Niyat, and A.R. Niknam, Phys. Plasmas, **23**, 062102 (2016). https://doi.org/10.1063/1.4953094
[26] S.M. Khorashadizadeh, E. Rastbood, and A.R. Niknam, Phys. Plasmas, **22**, 072103 (2015). https://doi.org/10.1063/1.4926521
[27] M.S. dos Santos, L.F. Ziebell, and R. Gaelzer, Phys. Plasmas, **22**, 122107 (2015). https://doi.org/10.1063/1.4936972
[28] P. Verma, and M.S. Tiwari, Physica Scripta, **44**, 296 (1991). https://doi.org/10.1088/0031-8949/44/3/010
[29] J.D. Huba, J. Geophys. Res. **86**, 3653 (1981). https://doi.org/10.1029/JA086iA05p03653
[30] R.S. Pandey , Progress in Electromagnetics Research B, **11**, 39 (2009). https://www.jpier.org/PIERB/pierb11/04.08073101
[31] Eliasson, P.K. Shukla, and J.O. Hall, **13**, 024502 (2006). https://doi.org/10.1063/1.2173934.
[32] E.N. Opp, and A.B. Hassam, Phys. of Fluids B, **3**, 885 (1991). https://doi.org/10.1063/1.859845
[33] M. Fujimoto, and T. Terasawa, J. Geophys. Res. **100**, 12025 (1995). https://doi.org/10.1029/94JA02219
[34] N.F. Ness, et al. Science, **233**, 4759 (1986). https://doi.org/10.1126/science.233.4759.85
[35] S. Stanley, and J. Bloxham, Nature, **428**, 151 (2004). https://doi.org/10.1038/nature02376

ВИВЧЕННЯ ЕЛЕКТРОСТАТИЧНИХ ІОННО-ЦИКЛОТРОННИХ ХВИЛЬ У МАГНІТОСФЕРІ УРАНУ

Рама С. Пандей, Мукеш Кумар

[a]*Факультет прикладної фізики Інституту прикладних наук Аміті, Університет Аміті Нойда, Індія.*
[b]*Факультет фізики, Коледж Наланда Біхаршаріф Наланда MU Бодх Гая Біхар, Індія*

У цьому рукописі використано метод характеристик деталей траєкторій частинок та дисперсійне співвідношення для іоносфери Урана для дослідження електростатичних іонно-циклотронних хвиль із паралельним зсувом швидкості потоку за наявності перпендикулярного неоднорідного постійного електричного поля та градієнта щільності. Швидкість зростання розрахована за допомогою дисперсійного співвідношення. Електричні поля, паралельні магнітному полю, передають енергію, масу та імпульс в авроральних областях магнітосфери планети, прискорюючи заряджені частинки до надзвичайно високих енергій. Вважається, що на швидкість нагрівання частинок плазми вздовж і перпендикулярно магнітному полю також впливає виникнення іонних циклотронних хвиль і паралельного електричного поля в області прискорення.

Ключові слова: електростатичні іонно-циклотронні хвилі, швидкість зсуву, градієнт щільності та неоднорідне електричне поле, магнітосфера/іоносфера Урана